



Investigation of synthesized carbon nanofilaments by reactive magnetron reactive sputtering methane decomposition

¹Shaidalina D.R., ^{1*}Baitimbetova B.A., ²Astemessova K.S., ²Turlybekova G.K., ³Topanov B.G.,
⁴Bukhvalov D.V., ⁵Chuchvaga N.A., ⁵Mit' K.A., ⁶Serikkanov A.S.

¹Mining and Metallurgical Institute, Satbayev University, Almaty, Kazakhstan

²Institute of Energy and Mechanical Engineering, Satbayev University, Almaty, Kazakhstan

³The Institute of Combustion Problems Committee of Science of the Ministry of Education and Science of the Republic of Kazakhstan, Almaty

⁴College of Science, Institute of Materials Physics and Chemistry, Nanjing Forestry University, Nanjing, China

⁵Institute of Physics and Technology LLP, Satbayev University, Almaty, Kazakhstan

⁶National Academy of Sciences of the Republic of Kazakhstan under the President of the Republic of Kazakhstan, Almaty

*Corresponding author email: baitim@physics.kz

<p>Received: September 25, 2025 Peer-reviewed: November 17, 2025 Accepted: February 23, 2026</p>	<p>ABSTRACT This work presents the synthesis of carbon nanofilaments obtained through the decomposition of graphite in methane plasma with argon admixture. The resulting nanostructures exhibit an amorphous configuration and remain transparent across the visible spectrum, making them attractive candidates for optical and optoelectronic applications. Atomic force microscopy revealed that the filaments form a compact, vertically oriented network on the substrate surface, while Raman spectroscopy provided information on their local bonding environment. Morphologically, the carbon filaments display flattened, ribbon-like forms, and their densely packed columnar structures reach an average length of ~36 nm. The optical transmission spectrum showed transmittance of ~65% near 400 nm, ~75% within the visible region, and nearly 80% in the near-infrared range, gradually increasing toward longer wavelengths. This degree of transparency in the visible spectrum is sufficient for practical device applications. When the incident light wavelength is comparable to or smaller than the inter-filament spacing (100–500 nm), light propagation occurs through reflections from the filament walls. The optical band gap of the structures was determined to be ~2.85 eV. Overall, the analysis of structural and optical properties confirms the successful fabrication of amorphous carbon nanofilaments, highlighting their strong potential for integration into advanced optoelectronic systems.</p>
	<p>Keywords: reactive magnetron sputtering, nanofilaments, methane gas, thin film, nanostructure.</p>
Shaidalina Damira	<p>Information about authors: PhD student, Master of Engineering and Technology, Mining and Metallurgical Institute, Satbayev University, Satpayev str. 22, 050013, Almaty, Kazakhstan. Email: Shaidalina.D@stud.satbayev.university; ORCID ID: https://orcid.org/0009-0003-4734-170X</p>
Baitimbetova Bagila	<p>Candidate of Physical and Mathematical Sciences, Associate Professor, Mining and Metallurgical Institute, Satbayev University, Satpayev str. 22, 050013, Almaty, Kazakhstan. Email: baitim@physics.kz; ORCID ID: https://orcid.org/0000-0002-3728-2430</p>
Astemessova Kalamkas	<p>Doctor of PhD, Head of Department, Institute of Energy and Mechanical Engineering, Satbayev University, Satpayev str. 22, 050013, Almaty, Kazakhstan. Email: k.astemessova@satbayev.university; ORCID ID: https://orcid.org/0000-0002-4143-6084</p>
Turlybekova Gulzhan	<p>Candidate of technical sciences, Associate professor, Institute of Energy and Mechanical Engineering, Satbayev University, Satpayev str. 22, 050013, Almaty, Kazakhstan. Email: g.turlybekova@satbayev.university; ORCID ID: https://orcid.org/0000-0001-5522-4931</p>
Topanov Bolat	<p>Senior Research Scientist, The Institute of Combustion Problems Committee of Science of the Ministry of Education and Science of the Republic of Kazakhstan, 050012, Bogenbai Batyr str. 172, Almaty, Kazakhstan. Email: topikbotat@mail.ru; ORCID ID: https://orcid.org/0009-0008-7872-1437</p>
Danil Boukhvalov	<p>Candidate of Physical and Mathematical Sciences, College of Science, Institute of Materials Physics and Chemistry, Nanjing Forestry University, Nanjing, 210037, China. Email: danil@njfu.edu.cn; ORCID ID: https://orcid.org/0000-0002-2286-3443</p>
Chuchvaga Nikolay	<p>Doctor of PhD, Deputy Director of Institute for Scientific Work, Institute of Physics and Technology LLP, Satbayev University, 050032, Ibragimov Street str. 11, Almaty, Kazakhstan. Email: n.chuchvaga@satbayev.university; ORCID ID: https://orcid.org/0000-0003-4417-4996</p>
Kostya Mit'	<p>Candidate of Physical and Mathematical Sciences, Institute of Physics and Technology, Satbayev University, 050032, Ibragimov Street str. 11, Almaty, Kazakhstan. Email: k.mit@sci.kz; ORCID ID: https://orcid.org/0000-0002-0078-6723</p>
Serikkanov Abay	<p>Candidate of Physical and Mathematical Sciences, Professor, National Academy of Sciences of the Republic of Kazakhstan under the President of the Republic of Kazakhstan, 050010, Shevchenko street str.28, Almaty, Kazakhstan. Email: a.serikkanov@gmail.com; ORCID ID: https://orcid.org/0000-0001-6817-9586</p>

Introduction

In recent years, humanity has faced new challenges in organizing social and economic relations. History demonstrates that economic revolutions are frequently accompanied by scientific breakthroughs, where a qualitative shift emerges after the gradual accumulation of knowledge. Within the framework of our research, one of the tasks was to study carbonaceous residues obtained during experiments performed by reactive magnetron sputtering [1]. A review of the literature, combined with optical characterization of these residues, suggested that they represent heterogeneous carbon formations containing nanofibers. To properly follow the logic of this investigation, it is necessary to refer to relevant earlier studies [2].

The main aim of this work is to synthesize and investigate carbon nanofilaments of various architectures for different practical applications. In particular, we focused on amorphous carbon nanofilaments with broad optical transparency covering both the visible and near-infrared regions, which makes them promising for optoelectronic devices. Owing to their topology, carbon nanostructures often exhibit properties of quantum-size systems and are therefore of considerable scientific and technological interest. The nanofilament concept is widely applied across materials science, nanotechnology, and device engineering. For instance, nanofilaments can serve as fundamental elements in nanoscale electronics, such as nanowire transistors, where their unique nanoscale electronic properties can be fully exploited [[3], [4]].

Several studies have emphasized the fabrication of advanced nanostructures [5], including patterned metasurfaces [5] and the integration of ZnO nanofilaments into one-dimensional TiO₂ structures [6]. These publications primarily concentrate on synthesis techniques and subsequent analysis [6].

Reference [7] provides a comprehensive overview of how carbon nanofilaments have been integrated into cementitious composites. It also reports recent experimental results demonstrating improvements in the mechanical performance of CNF-reinforced cements [8].

There are three main approaches to fabricating such carbon nanostructures: arc discharge [[9], [10], [11], [12]], laser ablation [[10], [11], [12]], and chemical vapor deposition (CVD) [11]. For example, in [[10], [11], [12]], CNTs and CNFs were synthesized on an aluminum substrate pre-coated with nickel,

which acted as a catalyst (approximately 5 wt.%). Key parameters such as carrier gas composition, reaction temperature, and growth duration were shown to significantly affect the resulting morphology [12].

In another study, a ternary catalyst system consisting of NiO, CuO, and Al₂O₃ was designed with three distinct regions for the synthesis of CNTs and carbon nanosheets (CNSs). The process relied on thermal CVD with acetylene as the precursor [[10], [11], [12], [13]]. Reference [14] investigated carbon nanotubes and nanofilaments synthesized via catalytic acetylene decomposition over Pd/Al₂O₃ catalysts. At 700 °C, the products were predominantly CNFs with diameters in the 9–26 nm range, while at 800 °C, multiwalled CNTs with a layered morphology were formed. Under other conditions, amorphous carbon with diverse geometries was also observed.

One strategy to prevent aggregation of CNTs and CNFs is to anchor their ends, enabling the formation of stable hierarchical structures. A common approach involves growing CNTs directly on micron-sized carbon fibers. For example, CNTs have been deposited on both polyacrylonitrile- (PAN-) and pitch-based fibers using hot-filament CVD with H₂ and CH₄ as feed gases. In this case, nickel clusters electrodeposited onto the fiber surface served as catalysts, producing uniform coatings of multiwalled CNTs with smooth walls and low impurity levels [15].

Carbon nanofilaments and nanotubes show strong potential in enhancing the performance of fiber-reinforced polymer (FRP) composites by improving both mechanical behavior and multifunctionality. Direct dispersion of nanofilaments into the polymer matrix, however, has drawbacks. A promising alternative involves growing large volumes of aligned CNFs directly on

fiber surfaces before composite processing. The so-called *graphitic structures by design* (GSD) approach makes use of fuel mixtures and nickel catalysts, and has been shown to produce nanofilament coatings on commercial PAN-based fibers at 550 °C using ethylene as the carbon source [16].

The pyrolysis of methane, acetylene, and benzene has been extensively studied. Methane, unlike CO, does not easily decompose at low temperatures, which favors the growth of single-walled CNTs with fewer amorphous carbon impurities. Various activation methods have been tested, including external gas heating, plasma excitation (microwave plasma, glow discharge, etc.),

hot-filament techniques, and laser heating. The most common plasma synthesis route employs methane diluted with hydrogen [17].

Magnetron sputtering is also an important method in plasma nanotechnology, enabling the deposition of graphite films, nanotubes, and related carbon nanostructures [18]. Owing to their high strength and stiffness, CNFs/CNTs are regarded as effective reinforcements for cementitious materials [19]. Nevertheless, their direct incorporation presents practical challenges.

Catalytic methane decomposition (CDM) offers a CO₂-free hydrogen production pathway while yielding CNFs as valuable by-products. Studies have applied thermogravimetric screening to identify suitable catalysts by measuring carbon yield in CDM [20]. For example, Ni–Cu–Mg–Al catalysts have been tested, where Cu content was shown to affect both filament morphology and catalyst particle size [20]. Beyond catalytic methods, other synthesis approaches such as graphene growth and template-assisted methods are also employed [[21], [22]].

In [22], nanofilaments were synthesized directly on carbon fiber surfaces using GSD techniques, while liquid-phase carbonization with anodic alumina templates produced porous carbon structures. Samples annealed at 1000 °C exhibited higher electrochemical capacity compared to those treated at higher temperatures. Other works demonstrated multiscale growth of nanofilaments using Pd catalysts from ethylene/oxygen mixtures at 550 °C, producing filaments whose diameters corresponded to catalyst particle size [23]. These fibers showed potential for improving strength, ductility, and energy absorption in composite systems.

High-pressure synthesis of sp³-hybridized hydrogenated carbon nanofilaments remains an active field. Such materials are expected to possess superior strength due to their dense packing and strong covalent bonding. In one study, mechanochemical synthesis was used to transform benzene into crystalline bundles of sp³-carbon nanofilaments under uniaxial compression, with the resulting fibers demonstrating ease of exfoliation and high energy density [24]. Raman spectroscopy, XRD, SEM, and TEM analyses were used to study their structure and growth mechanisms.

The relationship between catalyst properties and filament texture was also reported in [25], where CNTs and CNFs were synthesized on Ni–Cu–Mg–Al catalysts via vapor-phase deposition. It was established that the graphene orientation and

crystalline domains in the filaments are directly correlated with the morphology and dimensions of the catalyst particles.

In the present work, we focus on amorphous, columnar carbon nanofilaments synthesized by plasma-assisted methane decomposition with argon addition. Their structural features, including transparency and vertical alignment, make them suitable for optoelectronic applications.

Experimental part

A. Method of magnetron sputtering

In this study, direct-current magnetron sputtering of a graphite target was employed under varying working gas pressures at room temperature. Magnetron sputtering is a widely used physical vapor deposition technique for producing thin films on a substrate. In this method, the target material, which simultaneously acts as the cathode, undergoes erosion under the influence of a magnetron plasma discharge. The process initiates with the generation of plasma within the chamber above the target surface, where accelerated electrons collide with inert gas atoms, typically argon, leading to ionization.

In the case of reactive magnetron sputtering, an additional reactive gas, methane, is introduced. This gas interacts with the sputtered atomic species during deposition, thereby facilitating the formation of a compound thin film. Depending on the process conditions, reactions may occur either directly on the target surface or predominantly at the substrate. When the partial pressure of the reactive gas is high, reactions take place at the target surface, producing compounds that are subsequently transported and deposited on the substrate. Conversely, at lower pressures, the interaction in the gas phase is limited, and the reactions primarily occur on the substrate surface as solid-phase processes.

During sputtering, positively charged argon ions generated within the plasma are accelerated toward the graphite cathode, impacting its surface and ejecting carbon atoms and clusters. These liberated species travel through the plasma toward the substrate, where they condense and form thin films. The high plasma current enhances decomposition, excitation, and ionization of methane molecules, resulting in a flux of energetic species, including free atoms with sufficient kinetic energy to surpass the activation barrier for diffusion and nucleation. As a

consequence, stable thin films of the desired material are formed on the substrate surface.

B. Carbon Nanofilaments fabrication

The coating deposition was carried out under fixed process conditions: the gas mixture consisted of 25% methane and 75% argon. The discharge parameters were maintained at a voltage of $U = 500$ V and a current of $I = 30$ mA, corresponding to a discharge power of $P = 15$ W. The pressure inside the working chamber was kept at 6×10^{-3} Torr, while the vacuum lamp operated at a voltage of $U = 2.4$ mV. The sputtering duration was 15 minutes, and the substrate temperature was stabilized at 230 °C. Quartz substrates were employed for the deposition process.

C. Physical methods

The synthesized carbon nanofilaments were examined using a set of complementary physical characterization techniques, including X-ray diffraction (XRD), scanning electron microscopy (SEM), and Raman spectroscopy. Optical transmission spectra of the samples were recorded with SF-256 UVI and Shumasu spectrophotometers over a spectral range of 160–1100 nm. The phase composition was analyzed using a PANalytical X'Pert MPD PRO X-ray diffractometer equipped with Cu-K α radiation, and the obtained patterns were identified by comparison with the JCPDS reference database.

Electron microscopy investigations were conducted on an MT-MDT Integra Prima system and a Jeol SPM 5200 scanning probe microscope fitted with NSC 37 AIBS cantilevers. Raman measurements were performed on an MT-MDT Integra Spectra spectrometer at room temperature. A 473 nm semiconductor laser (2.62 eV) with a $2 \mu\text{m}$ spot size was used to excite the spectra, ensuring sufficient illumination of the thin-film surface. The accuracy of phonon frequency determination was within ± 4 cm^{-1} , with an exposure time of 30 seconds. To minimize local heating and irradiation effects from the 1.5 mW laser, the measurements were performed in scanning mode at a velocity of approximately $10 \mu\text{m/s}$.

Results and Discussion

Atomic force microscopy (AFM) is a highly effective technique for investigating the surface structure of thin films, as it enables the determination of surface roughness from several micrometers down to fractions of a nanometer. AFM micrographs of the synthesized samples

demonstrated that the carbon nanofilaments grow in a densely packed arrangement, oriented almost perfectly perpendicular to the substrate surface (Figure 1a). Morphologically, the filamentous carbon structures resemble flattened, ribbon-like forms. The average length of the vertically aligned, columnar nanofilaments was measured to be approximately 36 nm (Figure 1b).

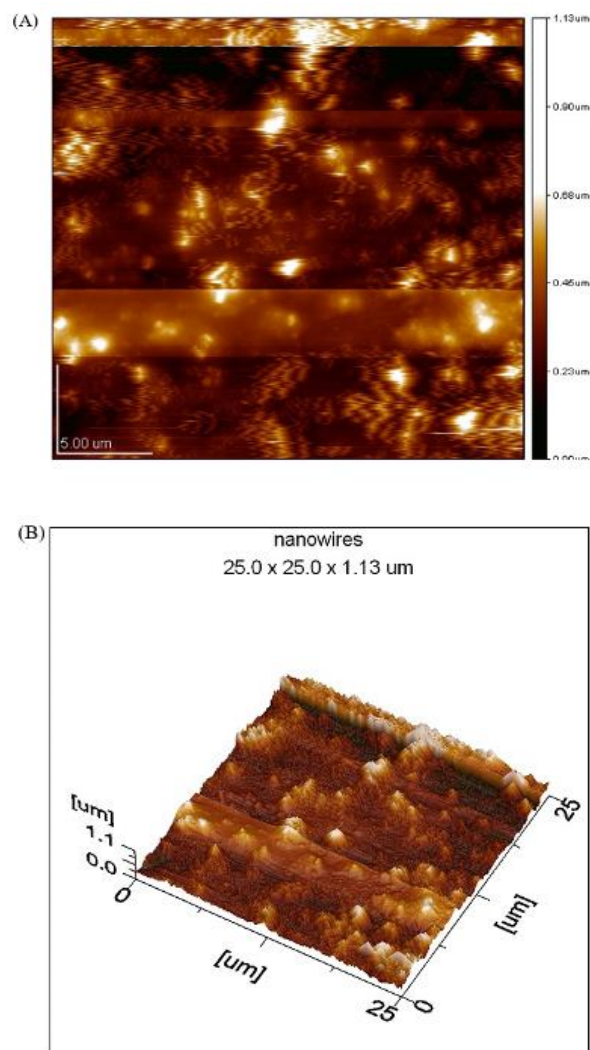


Figure 1 - AFM image of the nanofilament: (A) structure is a growth of densely packed nanofilaments strictly vertical to the substrate surface: (B) the columnar densely packed carbon nanofilament

The thickness of the deposited films was measured by comparing the cantilever displacement at regions without coating and at regions covered with the film. The height difference provided the film thickness, which was found to vary between $0.3 \mu\text{m}$ and $1 \mu\text{m}$. The synthesized nanofilaments reached lengths of up to 300 nm, with diameters ranging from 10 to 68 nm (Figure 2).

Initially, some uncertainty arose regarding the accuracy of these measurements. To ensure

reliability, AFM imaging was performed in two independent laboratories, using different instruments and specialized cantilevers designed for structures of this scale, thereby minimizing noise and measurement artifacts.

In order to study the optical characteristics of the nanocarbon structures, transmittance was measured with incident light directed perpendicularly to the sample surface. The obtained transmission spectrum, recorded within the 160–1100 nm range, is presented in Figure 3.

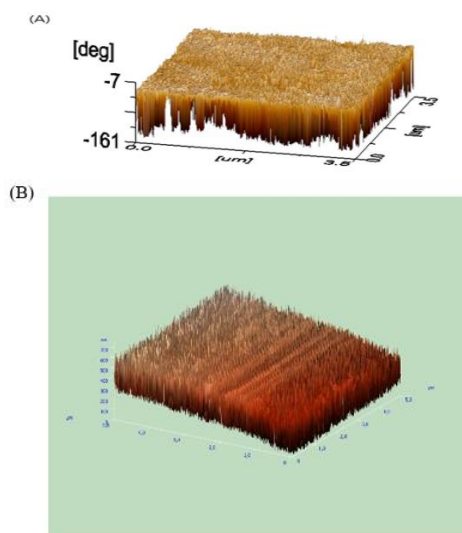


Figure 2 - Micrographs of carbon nanofilaments obtained in methane plasma, obtained by different atomic force microscopes:

- (A) Growth of carbon nanofilaments,
 (B) Arrays of vertically oriented carbon nanofilaments on quartz substrates.

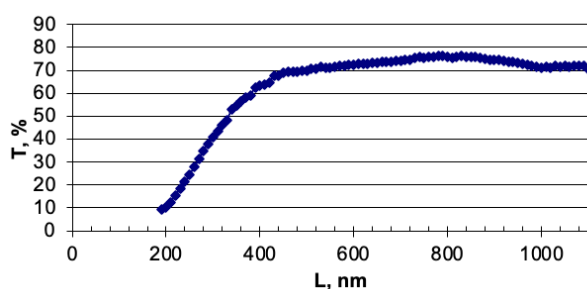


Figure 3 - Transmission spectrum of carbon nanofilaments

The transmission spectrum revealed that at a wavelength of approximately 400 nm (short-wavelength region), the transmittance reached about 65%. Within the visible range, the transparency remained around 75%, while in the near-infrared region it increased to nearly 80%, continuing to rise gradually with longer

wavelengths. Such a level of optical transparency in the visible spectrum is sufficient to enable the application of carbon nanofilaments in optoelectronic devices.

When the incident light wavelength is comparable to, or smaller than, the spacing between individual nanofilaments (100–500 nm), photons are able to propagate through the structure owing to multiple reflections from the filament walls. The optical band gap of the carbon nanofilaments was estimated to be approximately $E = 2.85$ eV. (Figure 4).

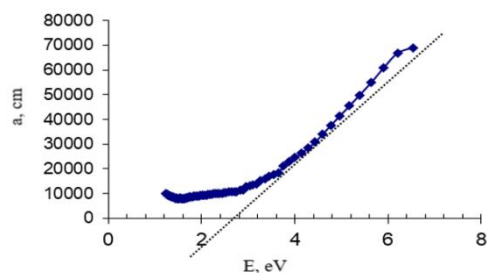


Figure 4 - Optical characteristics of the sample: dependence of a , on photon energy

The optical band gap of a bulk film, assumed to be homogeneous in mass, can be evaluated using the Bouguer–Lambert–Beer law, which defines the exponential relationship between light absorption and the electromagnetic wavelength [26]. For practical application, this general law can be reformulated into the following expression (1.1):

$$a = -\frac{\ln\left(\frac{\tau}{100}\right)}{\text{thickness}} \quad (1/cm) \quad (1.1)$$

Thickness $\approx 1000E-7$ cm

Raman spectroscopy is a highly informative technique for analyzing the vibrational modes and local structural environment of carbon-based materials, making it indispensable in their characterization. Disordered carbon films typically exhibit two characteristic features in their Raman spectra: the D-band (Disordered) in the range of 1350–1400 cm^{-1} , and the G-band (Graphitic) between 1575–1600 cm^{-1} . Variations in the relative intensities and frequency positions of these two peaks provide valuable insight into the degree of C–C bond hybridization and the evolution of allotropic modifications in the synthesized carbon films.

For crystalline graphite, Raman scattering generally produces two main bands: the G peak at ~ 1582 cm^{-1} , attributed to the doubly degenerate E_{2g} phonon mode within the graphene plane, and a low-

frequency feature near 42 cm^{-1} , associated with lattice vibrations involving sp^2 -hybridized carbon bonds [27]. Even slight disruptions of the graphite lattice can induce noticeable shifts in the G-band position. It has been reported [28] that when graphite crystallite sizes decrease to about 25 \AA , the G peak broadens and shifts to higher frequencies, up to 1593 cm^{-1} . In carbon nanostructures and nanotubes, multiple discrete vibrational modes may be detected within the G-band region (e.g., 1571 , 1585 , 1586 , 1587 , and 1593 cm^{-1}). For hollow carbon systems such as nanotubes of various morphologies, the Raman response becomes more complex, with additional peaks corresponding to different bonding environments.

The D-band, typically at $1341\text{--}1350\text{ cm}^{-1}$, arises from phonon modes near the M and K points of the Brillouin zone and is strongly correlated with structural disorder. These modes are particularly sensitive to lattice imperfections and are indicative of defect-induced vibrations. The G-band, spanning $1550\text{--}1594\text{ cm}^{-1}$, reflects the degree of order in graphitic materials and is used as a marker for structural organization in nanotubes and related systems. In contrast, the *2D (D) band**, observed in the $2500\text{--}2900\text{ cm}^{-1}$ region, originates from second-order resonant scattering involving two phonons of equal energy and opposite momentum near the K point. The intensity and profile of this band provide insight into the stacking and three-dimensional arrangement of graphene layers [[29], [30], [31], [32]].

The Raman spectra obtained for our carbon nanofilament samples are shown in Figure 5. The three most prominent lines typically observed in carbon materials were detected. The G peak at 1590 cm^{-1} corresponds to tensile vibrations of hexagonal carbon rings, associated with sp^2 bonding [35]. In amorphous carbon films, the G peak is often broadened and may shift within the $1500\text{--}1630\text{ cm}^{-1}$ range due to disordered bonding environments [34]. The D peak arises from breathing modes of hexagonal carbon units and is indicative of lattice disorder, influenced by phonons near the K point [[33], [34]]. Its absence suggests a lack of ring structures, as in pyrolytic graphite [[31], [32], [33], [34], [35], [36]].

The Raman spectrum of our samples (Figure 6) showed a dominant G peak at $\sim 1588\text{ cm}^{-1}$ with an associated shoulder in the low-frequency range, characteristic of amorphous carbon produced by reactive methane magnetron sputtering. The D line at 1350 cm^{-1} confirmed the presence of numerous defects. The 2D band ($2600\text{--}2710\text{ cm}^{-1}$) was also

detected, associated with two-phonon resonant scattering. The enhanced intensity of this band in certain regions suggests partial structural ordering within the amorphous carbon matrix.

For quantitative analysis, spectral deconvolution was carried out. Owing to the overlapping nature of the D and G peaks ($1000\text{--}1800\text{ cm}^{-1}$), Lorentzian fitting was employed, with additional verification using the Voigt function—a convolution of Lorentzian and Gaussian distributions. The fitting reliability exceeded 0.999, confirming the accuracy of the decomposition [[35], [36], [37]].

The structural classification of the films can thus be deduced from Raman spectral features. Narrow line widths ($20\text{--}40\text{ cm}^{-1}$) and the presence of both G and 2D peaks suggest a high degree of graphitization in certain domains, consistent with CNT-like regions. Furthermore, the intensity ratio I_D/I_G is strongly correlated with the lateral crystallite size (L_a), providing an estimate of the degree of disorder or graphitization in the films [[38], [39]]. The authors [[38], [39]] empirically derived the expression (1.2):

$$L_a\text{ (nm)} = 4.5R = 4.5 \cdot I_G / I_D \quad (1.2)$$

The lateral crystallite size (L_a) serves as an indicator of the structural type of carbon present in the sample. When $L_a > 20\text{ nm}$, the material exhibits predominantly graphitic characteristics. At $L_a \approx 10\text{ nm}$, the structure is classified as semi-graphitic, whereas values of $L_a \leq 5\text{ nm}$ correspond to amorphous carbon domains.

Raman scattering also provides the possibility to analyze spectra at different distances from the substrate surface, enabling the monitoring of structural variations along the vertical axis of the nanofilament array. In this study, it was demonstrated that the Raman response of vertically aligned nanofilaments exhibits noticeable changes depending on the position of the probing laser beam along their height, thereby reflecting spatial variations in structural ordering within the array.

Such an approach makes it possible to trace the structural evolution of nanofilaments throughout their vertical growth within the array. Recognizing these spectral variations provides a basis for controlling both the degree of ordering and the morphological profile of the synthesized nanofilaments, which is essential for tailoring their fabrication to specific applications. In this study, the key aspects of interpreting Raman spectra of light scattering from vertically aligned carbon nanofilament arrays have been outlined.

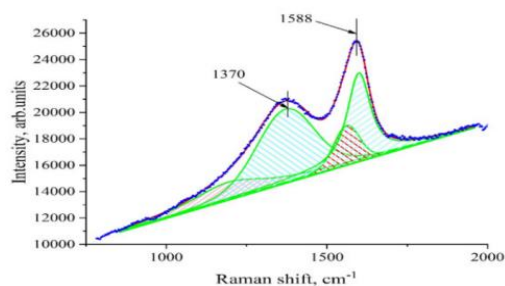


Figure 5 - Raman spectra of light scattering of the sample using the Voigt profile (Gaussian and Lorentz decomposition), carbon nanofilaments

Among the most informative techniques for characterizing crystalline structures, including nanostructured materials, is X-ray phase and structural analysis, which offers direct insight into lattice ordering and interplanar spacings. (Figure 6).

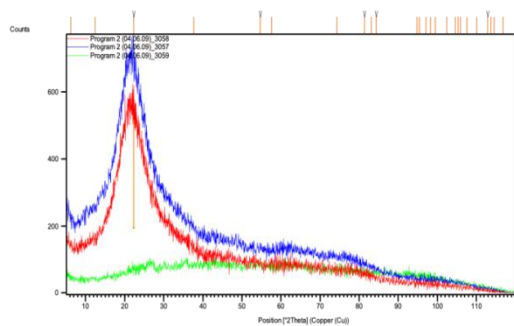


Figure 6- General view of the X-ray image of the nanofilament. a): Blue line by Bragg-Brentano method. Red line according to the sliding X-ray method. Green line by small angle X-ray scattering. Red line carbon on substrate quartz

The diffraction parameters of the carbon films deposited on quartz substrates—including the Bragg angles (2θ) of the X-ray reflections, line intensities (I), full width at half maximum (FWHM) of the peaks, and corresponding interplanar spacings (d)—are summarized in Table 1.

Based on the analysis of the X-ray peak broadening, the average size of amorphous crystallites was estimated to be approximately $L = 1.2 \text{ \AA}$, with an interplanar distance of $d = 3.98 \text{ \AA}$ (Table 1). The dominant reflection, observed at $2\theta = 22.28^\circ$, exhibited an integral intensity value of 100, confirming the presence of carbonaceous deposits within the sample.

A distinct category of nanostructured materials includes amorphous–crystalline systems and cluster-type metals and alloys, where crystalline domains are embedded within an amorphous matrix. In such cases, the characteristic dimensions

of the crystalline inclusions do not exceed 100 nm for amorphous–crystalline materials, while for cluster systems, the size of ordered regions is typically below 2 nm. Within the amorphous film matrix, these crystalline inclusions manifest as nanocrystals, thereby imparting unique structural and functional properties to the material [[40], [41]].

Table 1 - X-ray data of carbon nanofilaments

<i>Pos. [°2θ.]</i>	<i>d-spacing \AA</i>	<i>I, Int. [%]</i>	<i>FWHM [°2θ.]</i>
6.1907	14.26544	4.8	0.3
12.4479	7.10513	2.55	0.3
22.2838	3.98624	100	1.2
37.6532	2.38701	4.5	0.3
54.6909	1.67692	2.07	0.48
57.5956	1.59906	4.86	0.36
74.3308	1.27508	2.28	0.3
81.3617	1.18172	1.19	0.48
83.1549	1.16073	3.43	0.36
84.4011	1.14674	1.53	0.3
94.784	1.0466	2.61	0.36
95.491	1.04071	2.17	0.36
97.0905	1.02778	3.86	0.36
98.2354	1.01884	2.68	0.36
99.4839	1.00938	2.78	0.36
102.3854	0.9885	1.47	0.3
104.5484	0.97389	2.18	0.36
105.2722	0.96918	1.91	0.36
105.9447	0.96487	2.24	0.3
107.5544	0.95485	2.27	0.36
110.0735	0.93994	1.58	0.36
112.8789	0.92439	1.5	0.36
113.6632	0.92024	1.95	0.36
114.5307	0.91573	1.1	0.36
116.8588	0.90411	0.97	0.48

Conclusions

Carbon nanofilaments were successfully synthesized via reactive magnetron sputtering in a methane atmosphere. Raman spectroscopy revealed a distinct G-band at 1588 cm^{-1} for nanofilaments deposited on quartz substrates. Atomic force microscopy confirmed the formation of vertically aligned nanofilaments with diameters reaching up to 68 nm. X-ray diffraction analysis indicated that the average crystallite size was approximately $L = 1.2 \text{ \AA}$, with an interplanar distance

of $d = 3.98 \text{ \AA}$, and an integral peak intensity of 100 at $2\theta = 22.28^\circ$.

Optical transmission measurements demonstrated a transmittance of about 65% at 400 nm, approximately 75% across the visible region, and nearly 80% in the near-infrared range, showing a gradual increase at longer wavelengths. Such transparency within the visible spectrum is a critical property, highlighting the suitability of carbon nanofilaments for optoelectronic applications. Their ability to transmit visible light with minimal absorption or scattering is a key advantage for device integration.

Furthermore, a correlation was observed between the dimensions of nanofilaments composed of sp^2 nodes, the optical band gap, and the XRD results. The favorable conductivity of these structures, particularly in the direction perpendicular to the sputtering plane, suggests their potential use in perovskite solar cells. Specifically, they may serve as an intermediate layer preventing direct contact between silver electrodes and the p-layer of the perovskite absorber. As noted in [39], future advances in heterojunction photovoltaics are expected to exploit materials with quantum-dimensional effects, such as quantum wells and quantum barriers. In this context, the relative ease of fabricating carbon nanostructures could make

them an attractive candidate for further development in heterostructure-based solar technologies.

Conflict of Interest. The authors have no conflicts to disclose.

CRedit author statement: **D. Shaidalina:** Formal analysis, Data curation; **B. Baitimbetova:** Conceptualization, Methodology, Validation, Supervision, Investigation; **K. Astemessova:** Reviewing and Editing; **G. Turlybekova:** Data curation; **B. Topanov:** Methodology, Validation; **D. Bukhvalov:** Investigation, Formal analysis; **N. Chuchvaga:** Visualization, Writing, Reviewing and Editing; **Mit'**: Investigation; **A. Serikkanov:** Visualization.

Acknowledgments. This research was supported by the Research Grant from the Ministry of Science and Higher Education of the Republic of Kazakhstan.

Formatting of funding sources. AP32728461 - Development of technology for producing two-dimensional films based on graphene-containing structures and chalcogenide compounds for wide practical application, and BR28712683 - Development of a Technology for Reducing Energy Consumption and Waste Without Compromising Efficiency in the Recycling of Lithium-Ion Batteries.

Cite this article as: Shaidalina DR, Baitimbetova BA, Astemessova KS, Turlybekova GK, Topanov BG, Bukhvalov DV, Chuchvaga NA, Mit' KA, Serikkanov AS. Investigation of synthesized carbon nanofilaments by reactive magnetron reactive sputtering methane decomposition. *Kompleksnoe Ispolzovanie Mineralnogo Syra = Complex Use of Mineral Resources*. 2027; 343(4):34-45. <https://doi.org/10.31643/2027/6445.38>

Метанның ыдырауы кезінде реактивті магнетронды тозаңдату арқылы синтезделген көміртекті наноталшықтарды зерттеу

¹Шайдалина Д.Р., ¹Байтимбетова Б.А., ²Астемесова К.С., ²Турлыбекова Г.К., ³Топанов Б.А., ⁴Бухвалов Д.В., ⁵Чучвага Н.А., ⁵Мить К.А., ⁶Серикканов А.С.

¹Тау-кен-металлургия институты, Сәтбаев университеті, Алматы, Қазақстан

²Энергетика және машина жасау институты, Сәтбаев университеті, Алматы, Қазақстан

³Қазақстан Республикасы Білім және ғылым министрлігі Ғылым комитетінің Жану проблемалары институты, Алматы

⁴Ғылым колледжі, Материалдар физикасы және химия институты, Нанкин орман шаруашылығы университеті, Нанкин, Қытай

⁵ЖШС Физика-техникалық институты, Сәтбаев университеті, Алматы, Қазақстан

⁶Қазақстан Республикасы Президентінің жанындағы Қазақстан Республикасының Ұлттық ғылым академиясы

ТҮЙІНДЕМЕ

Бұл жұмыста графиттің метан плазмасында аргон енгізілуі арқылы ыдырауы нәтижесінде алынған көміртекті наноталшықтарды зерттеу нәтижелері келтірілген. Алынған наноталшықтардың аморфты құрылымы бар және көрінетін спектр аймағында мөлдірлігімен ерекшеленеді, бұл оларды оптикалық қолданбалар үшін болашағы бар екендігіне дәлел. Атомдық-күштік микроскопия көмегімен наноталшықтардың астар бетінде тығыз тік тор түзетіні анықталды. Үлгілердің жергілікті құрылымы Раман спектроскопиясы арқылы зерттелді. Морфологиялық тұрғыдан көміртекті талшық тәрізді құрылымдар жалпақ

<p>Мақала келді: 25 қыркүйек 2025 Сараптамадан өтті: 17 қараша 2025 Қабылданды: 23 ақпан 2026</p>	<p>таспа тәрізді түзілімдерге ұқсайды. Тығыз орналасқан колонна тәрізді көміртекті наноталшықтардың ұзындығы шамамен 36 нм құрайды. Тарату спектрі 400 нм шамасындағы қысқа толқынды аймақта тарату шамамен 65%-ға, көрінетін диапазонда шамамен 75%-ға жететінін, ал жақын инфрақызыл диапазонда ұзын толқын ұзындықтарында біртіндеп артуымен шамамен 80%-ға дейін артатынын көрсетеді. Көрінетін диапазондағы мөлдірліктің бұл деңгейі оптоэлектрондық құрылғыларда көміртекті наноталшықтарды пайдалану үшін жеткілікті. Түскен жарықтың толқын ұзындығы наноталшықтар арасындағы қашықтықпен (100–500 нм) немесе одан да қысқарақ болса, жарық олардың қабырғаларынан шағылысу арқылы олардың арасында тарай алады. Көміртекті талшықтың жолақ аралығы E=2,85 эВ. Сипаттама нәтижелерін талдағаннан кейін, көміртекті наноталшықтардың аморфты құрылымдармен тиімді синтезделгені туралы қорытынды жасауға болады, бұл олардың әлеуетін көрсетеді.</p>
<p>Шайдалина Дамира</p>	<p>Түйін сөздер: реактивті магнетронды шашырату, нано талшықтар, метан газы, жұқа қабықша, наноқұрылым.</p>
<p>Шайдалина Дамира</p>	<p>Авторлар туралы ақпарат: PhD докторанты, Техника және технологиялар магистрі, Тау-кен-металлургия институты, Сәтбаев университеті, Сәтбаев к-сі 22, 050013, Алматы, Қазақстан. Email: Shaidalina.D@stud.satbayev.university; ORCID ID: https://orcid.org/0009-0003-4734-170X</p>
<p>Байтимбетова Бағила</p>	<p>Физика-математика ғылымдарының кандидаты, қауымдастырылған профессор, Тау-кен-металлургия институты, Сәтбаев университеті, Сәтбаев к-сі 22, 050013, Алматы, Қазақстан. Email: baitim@physics.kz; ORCID ID: https://orcid.org/0000-0002-3728-2430</p>
<p>Астемесова Каламкас</p>	<p>PhD докторы, Кафедра меңгерушісі, Энергетика және машина жасау институты, Сәтбаев университеті, Сәтбаев к-сі 22, 050013, Алматы, Қазақстан. Email: k.astemesova@satbayev.university; ORCID ID: https://orcid.org/0000-0002-4143-6084</p>
<p>Турлыбекова Гулжан</p>	<p>Техникалық ғылымдар кандидаты, қауымдастырылған профессор, Энергетика және машина жасау институты, Сәтбаев университеті, Сәтбаев к-сі 22, 050013, Алматы, Қазақстан. Email: g.turlybekova@satbayev.university; ORCID ID: https://orcid.org/0000-0001-5522-4931</p>
<p>Топанов Болат</p>	<p>Аға ғылыми қызметкер, Қазақстан Республикасы Білім және ғылым министрлігі Ғылым комитетінің Жану проблемалары институты, 050012, Бөгенбай батыр к-сі 172, Алматы, Қазақстан. Email: topikbotat@mail.ru; ORCID ID: https://orcid.org/0009-0008-7872-1437</p>
<p>Бухвалов Данил</p>	<p>Физика-математика ғылымдарының кандидаты, Ғылым колледжі, Материалдар физикасы және химия институты, Нанкин орман шаруашылығы университеті, 210037, Нанкин, Қытай. Email: daniel@njfu.edu.cn; ORCID ID: https://orcid.org/0000-0002-2286-3443</p>
<p>Чучвага Николай</p>	<p>PhD докторы, директордың ғылыми жұмыс жөніндегі орынбасары, Физика-техникалық институты ЖШС, Сәтбаев университеті, Ибрагимова к-сі 11, Алматы, Қазақстан. Email: n.chuchvaga@satbayev.university; ORCID ID: https://orcid.org/0000-0003-4417-4996</p>
<p>Мить Костя</p>	<p>Физика-математика ғылымдарының кандидаты, Физика-техникалық институты ЖШС, Сәтбаев университеті, Ибрагимова к-сі 11, Алматы, Қазақстан. Email: k.mit@sci.kz; ORCID ID: https://orcid.org/0000-0002-0078-6723</p>
<p>Серикканов Абай</p>	<p>Физика-математика ғылымдарының кандидаты, профессор, Қазақстан Республикасы Президентінің жанындағы Қазақстан Республикасының Ұлттық ғылым академиясы, 050010, Шевченко к-сі 28, Алматы, Қазақстан. Email: a.serikkanov@gmail.com; ORCID ID: https://orcid.org/0000-0001-6817-9586</p>

Исследование синтезированных углеродных нановолокон методом реактивного магнетронного распыления при разложении метана

¹Шайдалина Д.Р., ¹Байтимбетова Б.А., ²Астемесова К.С., ²Турлыбекова Г.К., ³Топанов Б.А., ⁴Бухвалов Д.В., ⁵Чучвага Н.А., ⁵Мить К.А., ⁶Серикканов А.С.

¹ Горно-металлургический институт, Satbayev University, Алматы, Казахстан

² Институт энергетики и машиностроения, Satbayev University, Алматы, Казахстан

³ Институт проблем горения Комитета науки Министерства образования и науки Республики Казахстан, Алматы

⁴ Научный колледж, Институт физики и химии материалов, Нанкинский лесотехнический университет, Нанкин, Китай

⁵ ТОО Физико-технический институт, Satbayev University, Алматы, Казахстан

⁶ Национальная академия наук Республики Казахстан при Президенте Республики Казахстан

Поступила: 25 сентября 2025
Рецензирование: 17 ноября 2025
Принята в печать: 23 февраля 2026

АННОТАЦИЯ

В данной работе представлены результаты получения углеродных нановолокон путем разложения графита в метановой плазме с введением аргона. Полученные нановолокна имеют аморфную структуру и прозрачность в видимой области спектра, что делает их перспективными для оптических применений. Атомно-силовая микроскопия показала, что нановолокна образуют плотную вертикальную сетку на поверхности подложки. Локальная структура образцов была исследована с помощью рамановской спектроскопии. Морфологически углеродные нитевидные структуры напоминают плоские лентообразные

	<p>образования. Длина столбчатых, плотно упакованных углеродных нановолокон составляет около 36 нм. Спектр пропускания показывает, что в области коротких волн около 400 нм пропускание достигает около 65%, в видимом диапазоне — около 75%, а в ближнем инфракрасном диапазоне оно увеличивается до почти 80% с постепенным ростом на более длинных волнах. Такой уровень прозрачности в видимом диапазоне достаточен для применения углеродных нановолокон в оптоэлектронных устройствах. Когда длина волны падающего света сопоставима с расстоянием между нановолокнами (100–500 нм) или меньше его, свет может распространяться между ними за счет отражения от их стенок. Ширина запрещенной зоны углеродного нити составляет $E = 2,85$ эВ. После анализа результатов характеристики можно сделать вывод, что углеродные нанонити были эффективно синтезированы с аморфными структурами, что свидетельствует об их потенциале.</p>
	<p>Ключевые слова: реактивное магнетронное распыление, нано-нити, метановый газ, тонкая плёнка, наноструктура.</p>
Шайдалина Дамира	<p>Информация об авторах: PhD докторант, Магистр техники и технологии, Горно-металлургический институт, Satbayev University, 050013, ул.Сатпаева 22, Алматы, Казахстан. Email: Shaidalina.D@stud.satbayev.university; ORCID ID: https://orcid.org/0009-0003-4734-170X</p>
Байтимбетова Багила	<p>Кандидат физико-математических наук, ассоциированный профессор, Горно-металлургический институт, Satbayev University, 050013, ул. Сатпаева 22, Алматы, Казахстан. Email: baitim@physics.kz; ORCID ID: https://orcid.org/0000-0002-3728-2430</p>
Астемесова Каламкас	<p>Доктор PhD, Заведующая кафедрой, Институт энергетики и машиностроения, Satbayev University, 050013, ул. Сатпаева 22, Алматы, Казахстан. Email: k.astemessova@satbayev.university; ORCID ID: https://orcid.org/0000-0002-4143-6084</p>
Турлыбекова Гулжан	<p>К.э.н., ассоциированный профессор, Институт энергетики и машиностроения, Satbayev University, 050013, ул. Сатпаева 22, Алматы, Казахстан. Email: g.turlybekova@satbayev.university; ORCID ID: https://orcid.org/0000-0001-5522-4931</p>
Топанов Болат	<p>Ведущий научный сотрудник, Институт проблем горения Комитета науки Министерства образования и науки Республики Казахстан, 050012, ул. Богенбай батыра, 172, Алматы, Казахстан. Email: topikbotat@mail.ru; ORCID ID: https://orcid.org/0009-0008-7872-1437</p>
Бухвалов Данил	<p>Кандидат физико-математических наук, Научный колледж, Институт физики и химии материалов, Нанкинский лесотехнический университет, 210037, Нанкин, Китай. Email: daniel@njfu.edu.cn; ORCID ID: https://orcid.org/0000-0002-2286-3443</p>
Чучвага Николай	<p>Доктор PhD, Заместитель директора по научной работе, ТОО Физико-технический институт, Satbayev University, 050013, ул. Ибрагимова 11, Алматы, Казахстан. Email: n.chuchvaga@satbayev.university; ORCID ID: https://orcid.org/0000-0003-4417-4996</p>
Мить Костя	<p>Кандидат физико-математических наук, ТОО Физико-технический институт, Satbayev University, 050013, ул. Ибрагимова 11, Алматы, Казахстан. Email: k.mit@sci.kz; ORCID ID: https://orcid.org/0000-0002-0078-6723</p>
Серикканов Абай	<p>Кандидат физико-математических наук, профессор, Национальная академия наук Республики Казахстан при Президенте Республики Казахстан, 050010, ул. Шевченко 28, Алматы, Казахстан. Email: a.serikkanov@gmail.com; ORCID ID: https://orcid.org/0000-0001-6817-9586</p>

References

- [1] Baitimbetova BA, Vermenichev BM, Ryabikin YuA, Mansurov ZA, Abdikasova AA. Study of graphene formed in the atmosphere of vapors of aromatic hydrocarbons. Russian Physics Journal. 2015; 58(3):347-353. <https://doi.org/10.1007/s11182-015-0513-x>
- [2] Babu Naidu ChK, Kumar SN, Banerjee P. A review on the origin of nanofibers/nanorods structures and applications. Journal of Materials Science: Materials in Medicine. 2021; 32(6):68. <https://doi.org/10.1007/s10856-021-06513-4>
- [3] Torres-Costa V. Nanostructures for photonics and optoelectronics. Nanomaterials. 2022; 12:1820. <https://doi.org/10.3390/nano12101820>
- [4] Husain Z. (ed.). Emerging Trends in Nanotechnology. Springer Nature Singapore. 2021. <https://doi.org/10.1007/978-981-15-9904-0>
- [5] Huo D, Ma X, Su H, Wang C, Zhao H. Broadband absorption based on thin refractory titanium nitride patterned film metasurface. Nanomaterials. 2021; 11:1092. <https://doi.org/10.3390/nano11051092>
- [6] Liang Y, Zhao W. Crystal growth and design of disk/filament ZnO-decorated 1D TiO₂ composite ceramics for photoexcited device applications. Nanomaterials. 2021; 11:667. <https://doi.org/10.3390/nano11030667>
- [7] Байтимбетова БА, Рыабикин ЮА. Исследование углеродных наноструктур методом спектроскопии в карбонизованном феррохромовом шпеле [The study by spectroscopy method of carbon nanostructure in carbonized ferrochromic spinel]. Spectroscopy Letters. 2008; 41:9-14. (in Russ.). <https://doi.org/10.1080/00387010801905219>
- [8] Sobolev K, Shah SP. Nanotechnology in Construction. Proceedings of the 5th International Symposium on Nanotechnology in Construction (NICOM5). 2015.

- [9] Sharma R, Sharma AK, Sharma V. Synthesis of carbon nanotubes by arc-discharge and chemical vapor deposition method with analysis of its morphology, dispersion and functionalization characteristics. *Cogent Engineering*. 2015; 2:1-14. <https://doi.org/10.1080/23311916.2015.1061726>
- [10] Chrzanowska J, Hoffman J, Małolepszy A, Mazurkiewicz M, Stobiński L. Synthesis of carbon nanotubes by the laser ablation method: Effect of laser wavelength. *Physica Status Solidi (b)*. 2015; 252(8):1860-1867. <https://doi.org/10.1002/pssb.201552017>
- [11] Song L, Holleitner WA, Qian H, Hartschuh A. A carbon nanofilament-bead necklace. *Journal of Physical Chemistry C*. 2008; 112(26):9644-9649. <https://doi.org/10.1021/jp801608r>
- [12] Zhao N, Zhang Q, Wang J, Tian L, Qi Z, He F, Li Y. Synthesis of carbon nanostructures with different morphologies by CVD of methane. *Materials Science and Engineering A*. 2007; 460-461:255-260. <https://doi.org/10.1016/j.msea.2007.01.121>
- [13] Sivamaran VV, Balasubramanian M, Gopalakrishnan V, Viswabaskaran A. Combined synthesis of carbon nanospheres and carbon nanotubes using thermal chemical vapor deposition process. *Chemical Physics Impact*. 2022; 4:100072. <https://doi.org/10.1016/j.chphi.2022.100072>
- [14] Torres D, Pinilla JL, Suelves I. Screening of Ni-Cu bimetallic catalysts for hydrogen and carbon nanofilaments production via catalytic decomposition of methane. *Applied Catalysis A: General*. 2018; 559:10-19. <https://doi.org/10.1016/j.apcata.2018.04.004>
- [15] Lee SY, Yamada M, Miyake M. Synthesis of carbon nanotubes and carbon nanofilaments over palladium supported catalysts. *Science and Technology of Advanced Materials*. 2005; 6(4):420-426. <https://doi.org/10.1016/j.stam.2005.02.004>
- [16] Tehrani M, Boroujeni AY, Luhrs C, Phillips J, Al-Haik MS. Hybrid composites based on carbon fiber/carbon nanofilament reinforcement. *Materials*. 2014; 7(6):4182-4195. <https://doi.org/10.3390/ma7064182>
- [17] Zhao S, Hong R, Luo Z, Lu H, Yan B. Carbon nanostructures production by AC arc discharge plasma process at atmospheric pressure. *Journal of Nanomaterials*. 2011; 2011:346206. <https://doi.org/10.1155/2011/346206>
- [18] Yazdanbakhsh A, Grasley Z, Tyson B, Al-Rub RKA. Challenges and benefits of utilizing carbon nanofilaments in cementitious materials. *Journal of Nanomaterials*. 2012; 2012:371927. <https://doi.org/10.1155/2012/371927>
- [19] Dussault L, Pinilla JL, Suelves I, Moliner R, Lázaro MJ. New Ni–Cu–Mg–Al-based catalysts preparation procedures for the synthesis of carbon nanofibers and nanotubes. *Journal of Physics and Chemistry of Solids*. 2006; 67(5-6):1162-1167. <https://doi.org/10.1016/j.jpcs.2006.01.022>
- [20] Luhrs CC, Garcia D, Tehran M, Al-Haik M, Taha MR, Phillips J. Generation of carbon nanofilaments on carbon fibers at 550 °C. *Carbon*. 2009; 47(13):3071-3078. <https://doi.org/10.1016/j.carbon.2009.06.019>
- [21] Baitimbetova BA, Ryabikin YA. & Mukashev BN. Correction to: Study of Paramagnetic Properties of Graphene Structures Obtained from Pure Graphite in Organic Reagents Exposed to Ultrasound. *Russ Phys J*. 2021; 64:1582. <https://doi.org/10.1007/s11182-021-02494-0>
- [22] Xiang L, Zhang L, Xu T, Ding F, Yang W, Xu Y, et al. Mechanochemical synthesis of carbon nanothread single crystals. *Journal of the American Chemical Society*. 2017; 139(45):16343-16349. <https://doi.org/10.1021/jacs.7b08176>
- [23] Lee TW, Lee GH. Interstitial nanofilament pathway reduces energy consumption in memristors. *Nat. Nanotechnol*. 2025; 20:1552–1553. <https://doi.org/10.1038/s41565-025-02014-y>
- [24] Zeng Z, Natesan K. Relationship between the growth of carbon nanofilaments and metal dusting corrosion. *Chemistry of Materials*. 2005; 17(15):3794-3801. <https://doi.org/10.1021/cm050333a>
- [25] Monthieux M, Charlier JC, Masin F, Flahaut E, Razafinimanana M, Capria E, et al. Texturizing and structuring mechanisms of carbon nanofilaments during growth. *Journal of Materials Chemistry*. 2007; 17(46):4611-4623. <https://doi.org/10.1039/b708354a>
- [26] Sivukhin DV. Absorption of light and broadening of spectral lines. In: *General course of physics*. Moscow: Fizmatlit. 2005, 582-583. (in Russ.).
- [27] Nemanich RJ, Solin SA. First- and second-order Raman scattering from finite-size crystals of graphite. *Physical Review B*. 1979; 20(2):392-401. <https://doi.org/10.1103/PhysRevB.20.392>
- [28] Reich S, Thomsen C. Raman spectroscopy of graphite. *Philosophical Transactions of the Royal Society A*. 2004; 362(1824):2271-2288. <https://doi.org/10.1098/rsta.2004.1454>
- [29] Casimir D, Alghamdi H, Ahmed IY, Misra P. Raman spectroscopy of graphene, graphite and graphene nanoplatelets. In: Wongchoosuk Ch, Seekaew Y. (editors). *2D Materials*. London: IntechOpen. 2019. <https://doi.org/10.5772/intechopen.85711>
- [30] Ni Zh, Wang Y, Yu T, Shen Z. Raman spectroscopy and imaging of graphene. *Nano Research*. 2008; 1(4):273-291. <https://doi.org/10.1007/s12274-008-8036-1>
- [31] Mohiuddin TMG, Lombardo A, Nair RR, Bonetti A, Savini G, Jalil R, Bonini N, Basko DM, Galotit C. Uniaxial strain in graphene by Raman spectroscopy: G peak splitting, Grüneisen parameters, and sample orientation. *Physical Review B*. 2009; 79(20):205433. <https://doi.org/10.1103/PhysRevB.79.205433>
- [32] Ferrari AC, Meyer JC, Scardaci V, Casiraghi C, Lazzeri M, Mauri F, et al. Raman spectrum of graphene and graphene layers. *Physical Review Letters*. 2006; 97(18):187401. <https://doi.org/10.1103/PhysRevLett.97.187401>
- [33] Robertson J. Diamond-like carbon (DLC) coatings: classification, properties, and applications. In: Rajak KD, Kumar A, Behera A. (eds). *Applied Sciences*. 2021; 11:4445. <https://doi.org/10.3390/app11104445>
- [34] Ferrari AC, Robertson J. Interpretation of Raman spectra of disordered and amorphous carbon. *Physical Review B*. 2000; 61(20):14095-14107. <https://doi.org/10.1103/PhysRevB.61.14095>
- [35] Ferrari AC, Robertson J. Resonant Raman spectroscopy of disordered, amorphous, and diamondlike carbon. *Physical Review B*. 2001; 64(7):075414. <https://doi.org/10.1103/PhysRevB.64.075414>

- [36] Ryaguzova AP, Nemkayeva RR, Guseinova NP. Vliyanie uslovii sinteza i nanostruktur olova na svoistva a-C:H<Sn> kompozitnykh plenok [Influence of the synthesis conditions and tin nanoparticles on the structure and properties of a-C:H<Sn> composite thin films]. *Semiconductors*. 2018; 52(10):1327-1333. (in Russ.). <https://doi.org/10.1134/S1063782618100182>
- [37] Bukunov KA, Vorobyeva EA, Chechenin NG. Osobennosti ramanovskikh spektral'nykh kharakteristik v massive vertikal'no orientirovannykh mnogoslainnykh uglerodnykh nanotrubok [Features of Raman spectra of light scattering in an array of vertically oriented multi-walled carbon nanotubes]. *BMU. Series 3. Physics. Astronomy*. 2022; 49-54. (in Russ.).
- [38] Heise HM, Lampen P, Kiefer W, Hildebrandt P, Janotta M, et al. Characterisation of carbonaceous materials using Raman spectroscopy: a comparison of carbon nanotube filters, single- and multi-walled nanotubes, graphitised porous carbon and graphite. *Journal of Raman Spectroscopy*. 2009; 40(3):344-353. <https://doi.org/10.1002/jrs.2145>
- [39] Murae T, Kagi H, Masuda A. Structure and chemistry of carbon in meteorites. In: Oya H. (ed). *Primitive Solar Nebula and Origin of Planets*. Tokyo: Terra Scientific Publishing Company. 1993.
- [40] Alemasova NV, Bugorskaya DI, Burkhovetsky VV, Volkova GK, Glazunova VA, Burkhovetsky MYu, Zelensky MY, Savoskin MV. Grafit oksid: osobennosti issledovaniya materiala fizicheskimi metodami [Graphite oxide: peculiarities of material investigation by physical methods]. *Experimental Studies of Nanoparticles, Nanosystems and Nanomaterials. Physical and Chemical Aspects of the Study of Clusters. Nanostructures and Nanomaterials*. 2023; 15:8. (in Russ.).
- [41] Ryabov AV, Okishev KY. *New metallic materials and methods of their production: textbook*. Chelyabinsk: South Ural State University Publishing House. 2007.
- [42] Chuchvaga N, Kireev V, et al. Development of hetero-junction silicon solar cells with intrinsic thin layer: A review. *Coatings*. 2023; 13(4):796. <https://doi.org/10.3390/coatings13040796>